Int. J. Electrochem. Sci., 17 **(2022)** Article Number: 220111, doi: 10.20964/2022.01.08

International Journal of
ELECTROCHEMICAL
SCIENCE
www.electrochemsci.org

Effect of natural inhibitors on microalloyed steel corrosion in E5 and E10 biofuels

I.Vasquez-Aguirre[1], *A. Torres-Islas*[1,*], *M.G. Valladares-Cisneros*[1], *J. Colin*[1] *and H. Martinez*[2]

[1] Facultad de Ciencias Químicas e Ingeniería , Universidad Autónoma del Estado de Morelos, Av. Universidad 1001, Col. Chamilpa, C.P. 62209, Cuernavaca, Morelos, México.
[2] Laboratorio de Espectroscopia, Instituto de Ciencias Físicas, Universidad Nacional Autónoma de México, A.P. 48-3, C.P. &2210, Cuernavaca - 62210, Morelos México.
[*]E-mail: alvaro.torres@uaem.mx

Received: 3 September 2021 / *Accepted:* 21 October 2021 / *Published:* 6 December 2021

In this study, two natural extracts were evaluated as corrosion inhibitors, O. Vulgare and M. Spicata, in sugar cane ethanol mixed with gasoline (E5 and E10 biofuels), which were in contact with X-70 microalloyed steel with different heat treatments. The electrochemical techniques used were potentiodynamic polarization and electrochemical impedance spectroscopy, and I_{corr} was used as an indicator of the corrosion level. The results indicated that the main corrosion mechanism under all conditions is continuous anodic dissolution, which results from concentration polarization. Also, it was found that the microstructure of steel plays a determining role in the inhibition mechanism, which is influenced by energetic reactions related to the Temkin isotherm and physisorption.

Keywords: Natural inhibitors, Biofuels, X-70 microalloyed steel, Corrosion resistance.

1. INTRODUCTION

In the last decades, the use of sugar cane ethanol fuel in gasoline as an oxygenating agent has increased. Some of the reasons for this increase have been the Kyoto protocol and the replacement of the octane enhancer methyl-tert-butyl ether by sugar cane ethanol in the United States. However, the use of sugar cane ethanol has significantly increased not only in the U.S.A. but also in other countries and regions, including India, Russia, Europe, and Central America [1-4]. The blends whose trend represents the greatest use are those that contain 5% and 10% sugar cane ethanol by volume in gasoline, respectively (E5 and E10 biofuels), because their use does not require specific modifications or optimizations (recalibration and component changes) in internal combustion engines [5]. However, the storage and transport of these mixtures require corrosion-resistant materials, as sugar cane ethanol

leads to the degradation and significant corrosion of many metals, including zinc, brass, copper, aluminum, and some types of steel [4]. Moreover, sugar cane ethanol absorbs significant amounts of water, which is one of the factors that promote its different corrosion mechanisms because of acidic substances and peroxides [4]. Therefore, corrosion inhibitors are added to these biofuels to reduce corrosion during storage and pipeline transportation and in car fuel tanks. Such inhibitors are widely used in the control and prevention of corrosion. However, most of the compounds used for this purpose are too toxic, expensive, and harmful to the environment and human beings [6,7]. Thus, it is necessary to find environmentally friendly, efficient, and cheap corrosion inhibitors. Plant extracts are biodegradable and represent a renewable source of chemical compounds with high potential as inhibitors [8]. When added in small concentrations to a corrosive medium, these substances slow or prevent the reactions between the metal and the medium. However, corrosion inhibitors are only effective for particular metallic materials in particular environments. Minor changes in the solution or alloy compositions can significantly alter the inhibition efficacy. Some publications [1-6, 9,10] have focused on studying the corrosion behavior and performance of the biofuels E10, E25, E40, E65, and E85, sugar cane ethanol and biodiesel when in contact with a variety of metallic and nonmetallic materials, including a variety of carbon steel and brass. However, there is relatively little information on the corrosion behavior of microalloyed steel and these types of biofuels. Also, there is no evidence of the study of natural extracts as corrosion inhibitors in this system, so the main objective of this work is to evaluate the corrosion behavior of X-70 microalloyed steels (as-received, quenched, and tempered steels) in E5 and E10 biofuels, respectively. In addition, two natural extracts (Menta spicata and Origanum vulgare) were employed as corrosion inhibitors. The analyses were done using electrochemical methods and adsorption isotherms. Overall, we believe that this study contributes to the sustainable and green performance of the global energy industry.

2. EXPERIMENTAL PROCEDURE

X-70 new microalloyed steel was employed, and Table 1 shows its chemical composition. In the as-received condition, the steel was obtained using a thermomechanical manufacturing process, resulting in a polygonal ferrite microstructure and perlite. Two heat treatments were done, as indicated in Table 2. The electrochemical cell experimental setup used for the potentiodynamic (PP) and electrochemical impedance spectroscopy (EIS) tests consists of X-70 steel samples encapsulated in an epoxy resin with an exposed area of 0.5 cm^2. The samples were abraded with 2000 grade SiC paper, polished with 1.0-micron alumina particles, washed with water, and finally degreased with acetone. At the end of the experiment, the samples were cleaned by dipping in distilled water for 5 min, followed by washing with acetone. A silver/silver chloride electrode (Ag/AgCl) was used as a reference electrode, and a graphite as an auxiliary electrode. The electrodes were connected to a Gill AC (ACM instruments) potentiostat controlled by a personal desktop computer. The test solutions were pure anhydrous and sugar cane ethanol, and E5 and E10 biofuels were prepared with 87 octane gasoline. The electrochemical tests were conducted for the steel under 3 conditions, (as-received, quenched and tempered) each of the samples immersed in the biofuels E5 and E10, respectively, and in pure sugar

cane ethanol, the extracts of Menta spicata and Origanum vulgare (M. Spicata and O. Vulgare), employed as corrosion inhibitors were added before each test in concentrations of 100, 150 and 300 ppm. The tests were performed at room temperature for time periods between 20-24 h, recording settle time in 8 to 9 h intervals (the "time") as well "before exposure" (time duration of a single test). The X-70 microstructures were characterized by a conventional metallographic technique and scanning electronic microscopy. For the EIS tests, the AC Gill potentiostat was calibrated according to the ASTM G106-89 Standard. The EIS test parameters were an AC current signal with an amplitude of 32 mV at an open circuit potential and in a frequency range of 30,000–0.01 Hz. The |Z| impedance modulus was employed by monitoring the corrosion behavior. PP tests were conducted following the recommendations of the ASTM G5-94 standard, and curves were performed at a sweep rate of 60 mV/min. The corrosion potential (E_{corr}) and corrosion density current (I_{corr}) values were employed in the corrosion behavior analysis. M. spicata and O. vulgare species were purchased in local market. The aerial parts were dried at room temperature in the laboratory and 100 g of each material sample were subjected to hydrodistillation for 5 h with 500 mL of distilled water using a Clevenger-type apparatus to obtain their essential oils. This step was repeated three times to obtain a considerable volume of each essential oil (2.5 mL) separately. Each essential oil was dried over anhydrous sodium sulfate and stored in sealed glass vials in a refrigerator at 4 °C until their use in corrosion inhibition experiments.

Table 1. Chemical composition of X-70 steel.

C	Mn	Si	P	S	Al	Nb	Cu	Cr	Ni	Mo	Ti	Fe
0.037	1.48	0.10	0.0098	0.0036	0.12	0.097	0.28	0.28	0.15	0.036	0.011	Bal

Table 2. X-70 heat treatments conditions.

Heat treatment	Conditions
Oil quenched	850°C, 40 min, oil quenched in static oil
Quenched and tempered	Oil quenched + 350°C for 30 min, furnace cooled

3. RESULTS AND DISCUSSION

3.1 Microstructures

The steel in the as-received condition, as shown in Fig. 1(a), exhibited a ferritic matrix with the presence of pearlite at the grain boundaries, and a fine dispersion of precipitates was found in the ferritic grains.

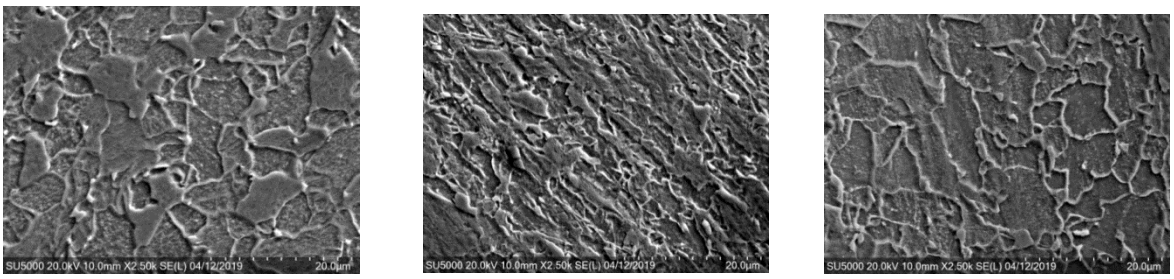

Figure 1. X-70 SEM steel microstructures: a) as-received, b) oil quenched, and c) tempered.

The microstructure of the tempered steel, as shown in Fig. 1b, showed an acicular ferrite matrix with the presence of martensite and pearlite grains (white) and retained austenite (gray), with a less number of precipitates in the ferritic grains than in the untreated steel. As shown in Fig. 1(c), the tempered steel showed a recrystallized ferrite matrix with isolated grains of cementite pearlite and a lower presence of retained austenite than the untreated steel, also exhibiting in isolated zones a fine dispersion of precipitates in the ferritic grains.

3.2 Heat treatment effects on the PP and EIS results in sugar cane ethanol

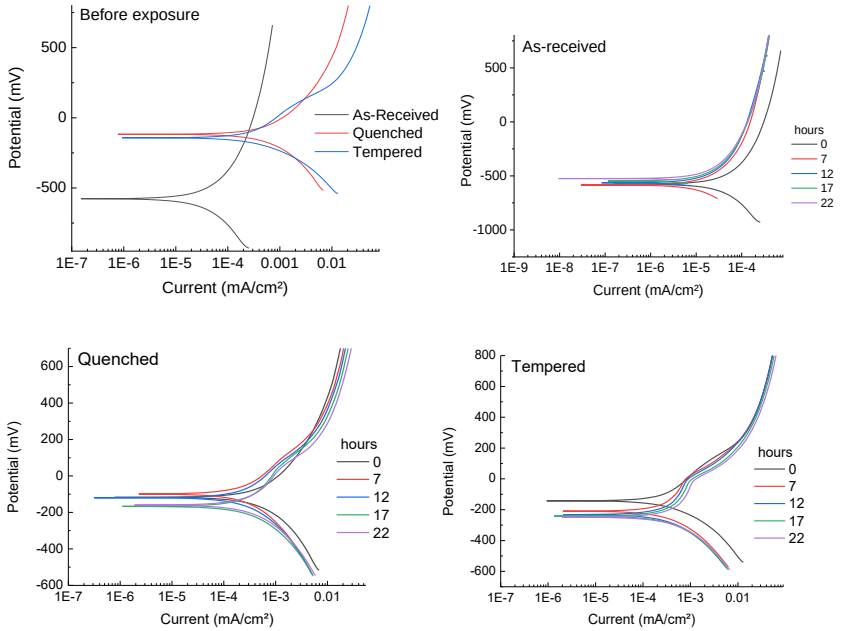

Figure 2. Potentiodynamic polarization curves before exposure and in time for as-received, quenched and tempered X-70 steel in contact with sugar cane ethanol at room temperature.

The results of the instantaneous potentiodynamic polarization tests on the steel in sugar cane ethanol in the three conditions are shown in Figure 2. It can be observed that for the three conditions, there was a corrosion mechanism by continuous anodic dissolution since the anodic branches of the curves did not show signs of passivation. The steel in the as-received condition presented the most cathodic value of E_{corr} in comparison with the other conditions, indicating that the equilibrium of the

cathodic and anodic reactions occurred for the as-received steel earlier than for the quenched and tempered steels, respectively. However, the tempered steel presented higher I_{corr} values of approximately one order of magnitude than the as-received steel. This behavior indicates that the microstructure of each of the conditions plays a very important role in I_{corr}. This statement is supported by the microstructural characteristics in each of the conditions, which, due to the phase difference, present galvanic micro pairs, and some of them are more reactive than others. As seen in Fig. 1a, the microstructure of the steel in the as-received condition mainly had ferrite with a presence of pearlite, in such a way that the cementite in the pearlite acted as a cathode that decreased the anodic reactions. On the contrary, the amount of the pearlitic phase decreased for the quenched and tempered steel, respectively. However, austenite and martensite had a relatively higher percentage of carbon than the as-received steel, which could also act as a cathode and decrease I_{corr}. There was little presence of ferrite and pearlite phases in the steel with these treatments. Due to the above behavior and the fact that the moisture or water content in sugar cane ethanol is practically null, the redox reactions did not present greater activity and did not generate protective oxides on the surface of the steel to protect it against corrosion or passivate it.

The potentiodynamic polarization tests as a function of time, as shown in the figures for all the conditions, showed the same behavior as the instantaneous tests, mainly due to the microstructural conditions, as mentioned above.

The Nyquist diagrams in Figure 3 show the steel behavior in the EIS tests under all conditions. It could be observed that the steel in the as-received condition in the initial tests and as a function of time presents a tendency to form a semicircle, which is related to the charge transfer mechanism, with impedance modulus (|Z|) values ranging from 1 MΩ to 2.5 MΩ. This charge transfer mechanism is mainly associated with a film of corrosion products on the material surface, which eventually generated passivation and a concentration of charges between the metal and the corrosive medium, presenting the double layer (dl) effect [11,12].

However, for the steel in the as-received condition, there was no indication of passivation, suggesting the presence of a charge concentration gradient between the metal and solution interface due to the ions generated by the redox reactions, which together with the low conductivity of the medium remained semistatic, gradually transferring electrons and protons. An opposite behavior occurred for the quenched and tempered steels, where a straight line was observed in the Nyquist diagrams with a tendency to form a 45-degree angle, which is mainly related to the ionic diffusion mechanism, presenting steel with a continuous dissolution behavior mainly due to the anodic activity of the present phases, as mentioned above.

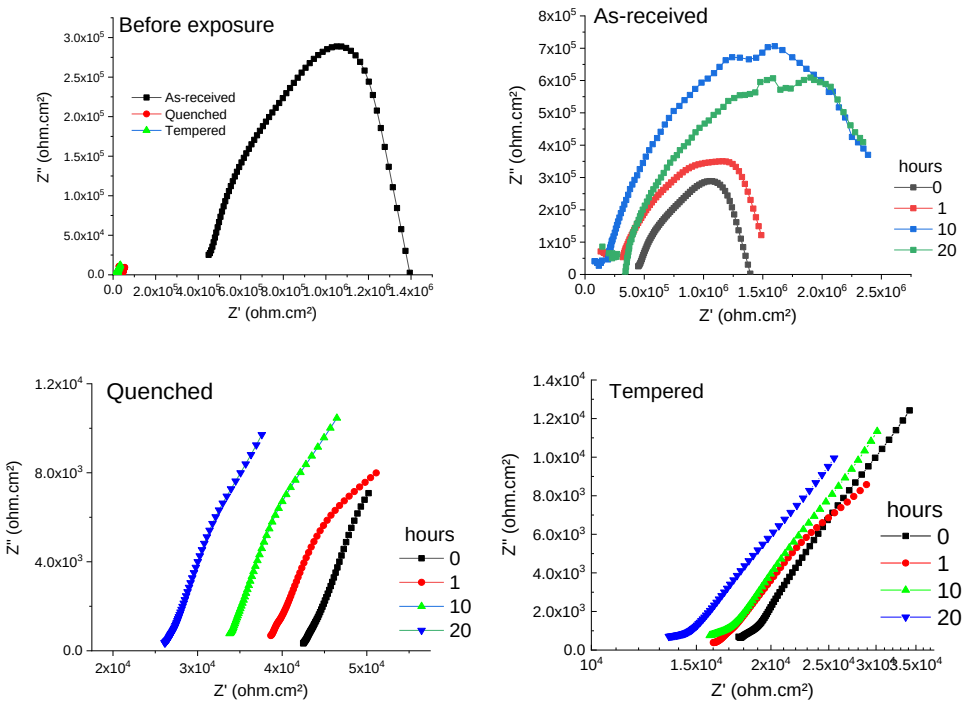

Figure 3. EIS curves before exposure and in time for as-received, quenched and tempered X-70 steel in contact with sugar cane ethanol at room temperature.

However, for the steel in the as-received condition, there was no indication of passivation, suggesting the presence of a charge concentration gradient between the metal and solution interface due to the ions generated by the redox reactions, which together with the low conductivity of the medium remained semistatic, gradually transferring electrons and protons. An opposite behavior occurred for the quenched and tempered steels, where a straight line was observed in the Nyquist diagrams with a tendency to form a 45-degree angle, which is mainly related to the ionic diffusion mechanism, presenting steel with a continuous dissolution behavior mainly due to the anodic activity of the present phases, as mentioned above.

3.3. Effects of the O. Vulgare and M. Spicata inhibitors extracts on the PP and EIS results in E5 and E10 biofuels

Through polarization curves, Figures 4 and 5 show the behaviors of the three kinds of steel when in contact with E5 biofuel without inhibitors extracts and with the two proposed inhibitors extracts (with different concentrations) before exposure and time tests. From these figures, it can generally be observed that the addition of gasoline to sugar cane ethanol did not change the continuous anodic dissolution behavior of steel. As suggested by Pedraza et al. [13], in gasoline- sugar cane ethanol mixtures, the water content in sugar cane ethanol is a determining factor in the passivation or dissolution process. However, the percentage of gasoline does affect the behavior of I_{corr}, which, as seen below, is presented in a similar way to E10 biofuel.

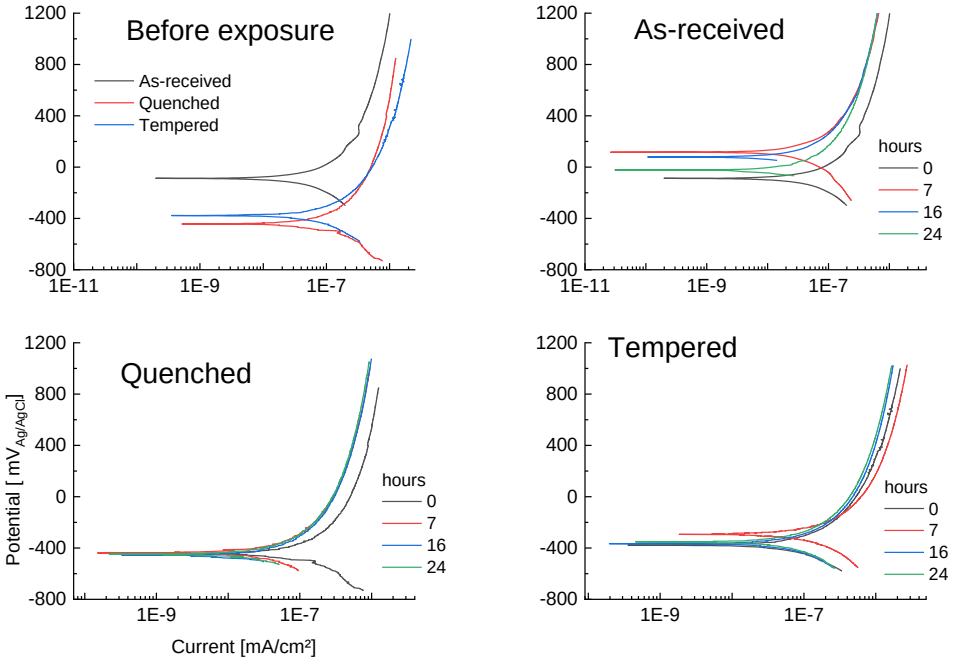

Figure 4. Potentiodynamic polarization curves before exposure and in time for as-received, quenched and tempered X-70 steel in contact with E5 biofuel without inhibitors extracts at room temperature.

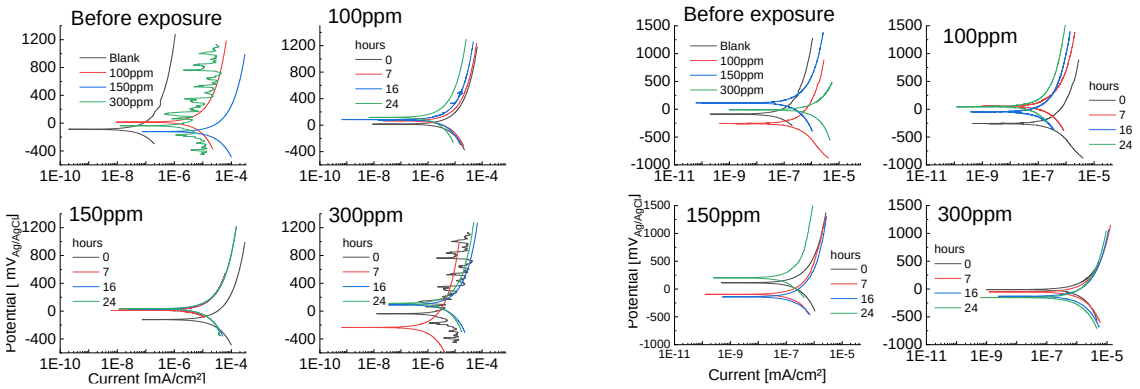

M. Spicata O. Vulgare

Figure 5. Potentiodynamic polarization curves before exposure and in time of X-70 steel in the as-received condition with E5 biofuel and 100,150 and 300 ppm inhibitors extracts M. Spicata and O. Vulgare, at room temperature.

The EIS tests indicated that although the polarization curves have similar behaviors, the addition of the inhibitors extracts resulted in different steel surface behaviors. This can be observed in the Nyquist and phase angle diagrams in Figure 6, where in comparison with the instantaneous tests and the concentrations of 100 and 300 ppm, the concentration of 150 ppm presents in an order of magnitude the highest values in Z', Z'' and |Z|. Only at 150 ppm concentration |Z| increased with the exposure time. This behavior occurred for the three kinds of steel, meaning that regardless of the phases present in the steel, the permanence mechanisms of both inhibitors extracts with 150 ppm are

similar, as well as for the instant immersed tests with 100 and 300 ppm. The above results indicate that both inhibitors extracts are anodic type inhibitors because in the polarization curves, I_{corr} decreased, and E_{corr} shifted to more positive values than 85 mV with the dwell time, thus blocking the anodic reactions [14].

Moreover, despite the capacitive behavior represented by the tendency to form semicircles in the Nyquist diagrams in Figure 6, the phase angle diagrams in the same figure generally present a constant decrease in the defacement angle at high frequencies (10000 Hz) from 80° to 0° and at low frequencies (0.01 Hz). This means that there is a charge concentration gradient between the metal surface and the solution, allowing ionic exchange toward the solution through a polarization mechanism primarily controlled by the concentration, where the changes in the system due to the different concentrations of the inhibitor extract increased or decreased the diffusion rate of the ions in the solution, eventually decreasing the polarization effects charge concentration gradient and increasing the corrosion rate according to the particular characteristics of this type of inhibitors.

It should be noted that in Figure 6, only the Nyquist diagrams for the O. Vulgare inhibitor extract and the phase angle diagrams for the M. Spicata inhibitor extract are presented, as the phase angle diagrams for the O. Vulgare inhibitor extract showed a similar behavior to the diagrams of the M. Spicata inhibitor extract.

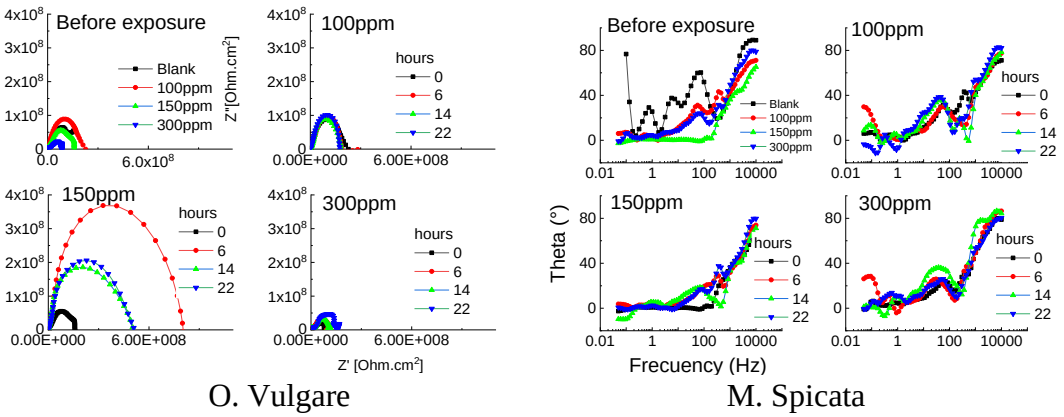

Figure 6. EIS curves before exposure and in time, of X-70 steel in the as-received condition with E5 biofuel and 100,150 and 300 ppm inhibitors extracts of M. Spicata and O. Vulgare, respectively at room temperature.

3.4. Steel heat treatment effects on the E_{corr}, I_{corr}, and $|Z|$ results in E5 and E10 biofuels with mint and oregano inhibitors extract

Figure 7 presents the graphs of the behaviors of the electrochemical parameters E_{corr}, I_{corr}, and $|Z|$ in E5 biofuel with the additions of O. Vulgare and M. Spicata inhibitors extracts, respectively, as a function of time.

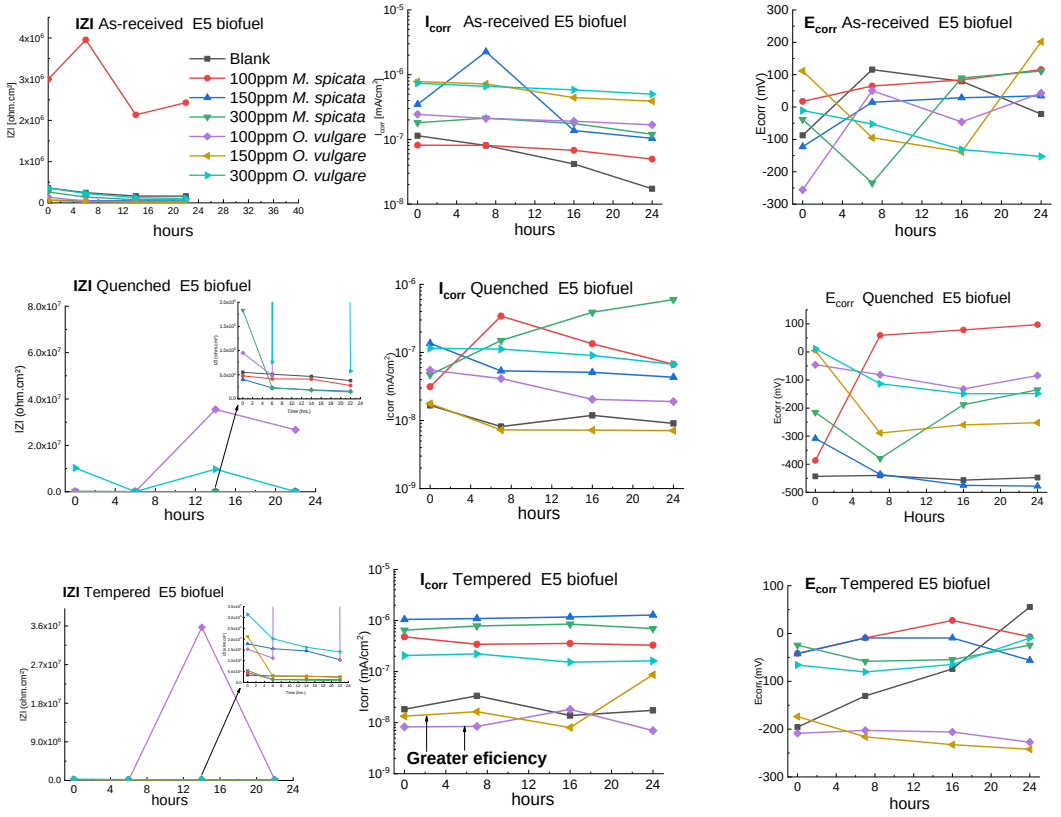

Figure 7. |Z|, I_{corr}, and E_{corr}, behavior in time, for as-received, quenched, and tempered X-70 steel when in contact with E5 biofuel and 100, 150 and 300 ppm inhibitors extracts M. Spicata and O. Vulgare, respectively at room temperature.

In this figure, it can be observed that the variations of |Z| and E_{corr} for all steels for both inhibitors extracts at the concentrations of 100, 150, and 300 ppm had random variations in their values, respectively, including the steel in contact with the biofuel without an inhibitor extract. As mentioned in the previous paragraphs, this is due to the anodic behavior of the inhibitors extracts. However, in the case without inhibitors extracts, the phases present in the steel and the galvanic micro pairs are the main reasons for this variation, which is less than that of the steel with an inhibitor extract. However, one of the main objectives of this study is to determine the test condition that decreases the corrosion level the most, for which the analysis of the corrosion current density I_{corr} provides a clear idea of the efficiency of the inhibitors extracts and their interactions with the different steel phases. In this figure, it can be observed that I_{corr} for the as-received steel with both inhibitors extracts generally had a tendency to increase between 1×10^{-6} and 1×10^{-7} compared to steel without an inhibitor extract. On the contrary, for the quenched steel, these levels decreased in the range of 1×10^{-7} and 1×10^{-8}, mainly with the addition of the inhibitor extract at 150 ppm of M. Spicata and at 100 and 150 ppm of O. Vulgare, respectively. 150 ppm of O. Vulgare presented the highest levels of inhibition after 8 hours of permanence. Additionally, in the same figure, it can be observed that heat treatment played an important role in the reduction of the corrosion levels, decreasing I_{corr} in an order of magnitude for the steels with the quenched and tempered treatments, where the tempered steel

showed to be most susceptible to generate the highest inhibition levels with the inhibitor extract O. Vulgare at 100 and 150 ppm, respectively. This combination of the heat treatment and inhibition extract achieved a two order of magnitude decrease in I_{corr} compared with the untreated and uninhibited steels. Table 3 illustrates the I_{corr} values as a function of the permanence time in detail.

Table 3. I_{corr} behavior in time of the X-70 tempered steel when in contact with E5 biofuel and 100 ppm inhibitor extract of O. Vulgare at room temperature.

Permanence time	As-received	Tempered steel (100ppm /O. Vulgare)	
0 h	1.83E-08	8.25E-09	
7 h	3.35E-08	8.44E-09	
24 h	1.74E-08	6.98E-09	**Decreasing trend**

The chemical compositions of the extracts of M. Spicata and O. Vulgare contained phenols and tannins. The presence of these phenols made these essences partially soluble since they are lipophilic and soluble in apolar organic solvents (hexane, ether, ethyl, etc.). Further, the solubility in alcohol is variable, but they are soluble in high-grade alcohols [15-19].

The presence of OH groups in tannins and phenols conferred them the capacity to form chelates and salts with the ferric ions and other metallic cations preferentially in the recrystallized ferrite matrix present in the tempered steel.

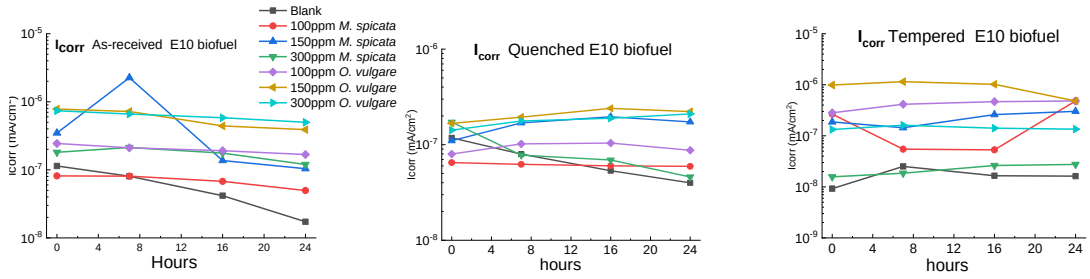

Figure 8. I_{corr} behavior in time of the as-received, quenched, and tempered X-70 steel when in contact with E10 biofuel and 100, 150 and 300 ppm inhibitor extracts O. Vulgare and M.Spicata at room temperature.

In addition, during the recrystallization process in the tempered steel, due to the increase in temperature, the dipoles formed were most likely susceptible to decompose into their constituent atoms to give rise to atomic agglomerations or "clusters" of nitrogen and carbon. Likewise, the concentration of the point defects or crystalline imperfections within the orthorhombic structure of cementite as a result of the plastic deformation caused this phase to be transformed into a nonstoichiometric compound with high energy values [20,21], thus, it facilitates the rapid dissolution and absorption of the inhibitor extracts complexes under study and cause the obstruction of microanodes, which are

generated on the metal surface when they come into contact with a corrosive medium, thereby delaying the steel dissolution [22,23].

Figure 8 only shows the I_{corr} behavior graphs for all steels with and without inhibitors extract at different concentrations and when in contact with E10 biofuel. The behavior in E_{corr} and |Z| respectively, practically presented in a similar way as with E5 biofuel. This indicates that both the inhibitors extracts in contact with E5 and E10 biofuels behaved in an anodic way, respectively, as previously explained. However, the difference in the conditions with E10 biofuel showed that regardless of the steel condition or the inhibitor's extract type and concentration, I_{corr} does not decrease compared to the steel without inhibitors extracts. On the contrary, the tendency is to increase the, which it is related to the gasoline concentration. E10 biofuel, which has the highest gasoline concentration promotes the dissolution of both inhibitors extracts by reducing the numbers of OH groups in the tannins and phenols that energetically interact with the different phases present in steel. The above idea is supported by the thermodynamic and kinetic electrochemical behaviors in the results of the potentiodynamic curves and Nyquist diagrams.

In addition, by adjusting the different adsorption isotherms, it was concluded that the main deposition mechanism of the inhibitors extracts on the steel surface is by the physical adsorption or physisorption corresponding to Temkin's adsorption isotherm model, (Fig.9) which is a spontaneous process where electrostatic interactions occur between the organic molecules of the medium and positive charges of the metal surface. This result confirms what was stated in the previous paragraphs.

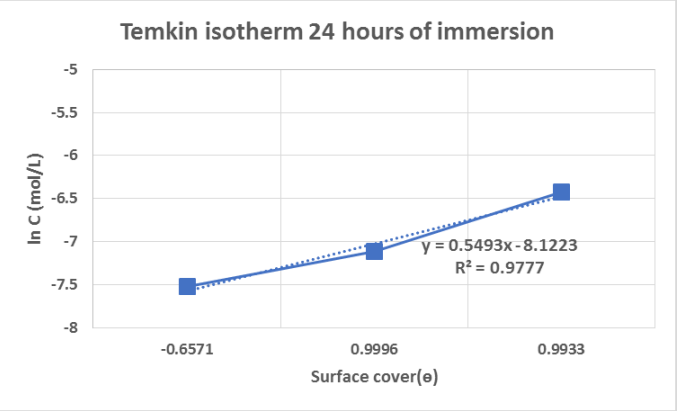

Figure 9. Experimental results of the Temkin adsorption isotherm for the O. vulgare inhibitor extract at different concentrations in E5 biofuel on X-70 tempered steel during 24 h of immersion.

4. CONCLUSIONS

1. Corrosion evaluation of X-70 microalloyed steels under three different conditions, as-received, quenched, and tempered, in contact with sugar cane ethanol, E5 and E10 biofuels were studied. The corrosion processes of the investigated samples present a continuous anodic dissolution mechanism, primarily attributed to the polarization due to the anodic and cathodic activities of the different phases present in the steels.

2. The results of the addition of the natural corrosion inhibitor extract, O. Vulgare, with concentrations of 100, 150, and 300 ppm to the three different steels indicated that it is an anodic type inhibitor whose best efficiency is for the tempered steel with a concentration of 100 ppm and when in contact with E5 biofuel. The corrosion level was decreased in two orders of magnitude in comparison with the steel without corrosion inhibitors extracts.

3. The results of the addition of the natural corrosion inhibitor extract M. Spicata with concentrations of 100, 150, and 300 ppm to the three different steels indicated that it is an anodic type inhibitor that does not decrease the corrosion level of steel when in contact with sugar cane ethanol and E5 and E10 biofuels. This is mainly due to the energetic mechanisms of inhibitors: dissolution and absorption.

4. The steel microstructure had a determining role in the corrosion mechanism and in the absorption of the natural corrosion inhibitors extracts, which are related to the galvanic micro pairs and particular crystalline imperfections in each of the present phases. Further, by means of the Temkin isotherm, it was determined that the main deposition mechanism of the extracts on the steel surface is physisorption.

References

1. J. Rawat, P.V.C. Rao and N.V. Choudary, *SAE* Number 2008-28-0125.
2. M.A. Ershov, E.V. Grigoreva, I.F. Habibullin, V.E. Emelyanov, D.M. Strekalina, *Renew. Sustain. Energy Rev.,* 66(2016)228.
3. J.R. Delfinoa, T.C. Pereira, H.D.C. Viegas, E.P. Marques, A.A.P. Ferreira, L. Zhang, J. Zhang, A.L.B. Marques, *Talanta*, 179(2018)753.
4. L. Matějovský, J. Macák, M. Pospíšil, M. Staš, P. Baroš, A. Krausova, *Energy Fuels*, 32(2018)5145.
5. M. De Sanctis, A. Dimatteo, G.F. Lovicu, D. Marc, R. Valentini, *La Metallurgia Italiana* 7-8(2010)33.
6. C. G. Dariva, A.F. Galio, Developments in Corrosion Protection, Chapter 16, INTECH, Croatia, 2014.
7. M. Chigondo, F. Chigondo, *J. Chem.,* Article ID 6208937, (2016), 7 pages.
8. I.B. Obota, D.D. Macdonalda, Z.M. Gasem, *Corros. Sci.,* 99(2015)1.
9. H. Jafari, M.H. Idris, A. Ourdjini, H. Rahimi, B. Ghobadian, *Mater. Corros.,* 61(2010)432.
10. J. Jiao, J. Li, Y. Bai, *J. Cleaner Prod.,* 180(2018)832.
11. C. Behnamian, A. Mostafaei, A. Kohandehghan, B.S. Amirkhiz, D. Serate, Y. Sun, S. Liu, E. Aghaie, Y. Zeng, M. Chmielus, W. Zheng, D. Guzonas, W. Chen, J. Li Luo, *Corros. Sci.,* 106(2016)188.
12. I. Nicic, D.D. Macdonald, *J. Nucl. Mater.,* 379(2008)54.
13. G.K. Pedraza-Basulto, A.M.A. Morquecho, J.A.C. Miramontes, A.B. Terrazas, A.M. Villafane, J.G.C. Nava*, Int. J. Electrochem. Sci.,* 8(2013)5421.
14. P.R. Roberge, Handbook of Corrosion Engineering, McGraw-Hill, USA, 2019.
15. J.Z. Mamani, “In vitro antibacterial activity of mint (Mentha piperita l.) essential oil against enteropathogenic escherichia coli (EPEC)”, Bachelor thesis dissertation, National University of the Altiplano, Puno, Peru, 2017.
16. E.E.M. Velázquez, K.R. Díaz, Ma.G.F.L. Piña, S.M. Díaz, R.R. Camacho, M.R. Gómez, *Rev. Mex. Cienc. Agríc.,* 3(2012)481.
17. E.A. Plaus, G.S. Flores, S.G. Ataucusi, *Rev. Med. Hered.*, 12(2001)16.

18. M.E.B. Oyarzabal, L.F.D. Schuch, L.D.S. Prestes, D.B.A. Schiavon, M.R.A Rodrigues, J.R.B. de Mello, *Rev. Cubana Plant. Med.,* 16(2011)260.
19. D. Acevedo, M. Navarro, L. Monroy, *Inf. Tecnol.,* 24(2013)43.
20. J. Languillaume, G. Kapelski, B. Baudelet, *Acta Mater*., 45(1997)1201.
21. A. Nahlé, I.A. Abdoun, I.A. Rahman, M.A. Khayat, *Int. J. Corros*., Article ID 460154(2010)9 pages.
22. B.E. Amitha Rani, B.B.J. Basu, *Int. J. Corros*., Article ID 380217(2012)15 Pages.
23. Y. El Aoufir, R. Aslam, F. Lazrak, R. Marzouki, S. Kaya, S. Skal, A. Ghanimi, I.H. Ali, A. Guenbour, H. Lgaz, I.M. Chung. *J. Mol. Liq.,* 303(2020)112631.